Malaya Journal of Matematik, Vol. 8, No. 2, 433-444, 2020

https://doi.org/10.26637/MJM0802/0018

Frequency analysis of Halo orbits in the Sun-Mercury system

Hemant Kumar Mishra[1]* and Govind Kumar Jha[2]

Abstract

Mercury is the planet which gains maximum radiation pressure from the Sun. On 20th October 2018 Bepicolombo was launched to do the comprehensive study of the magnetic field, magnetosphere, surface and internal structure of the Mercury. For this we need to maintain the nominal multi-revolution halo orbits. In this paper, we have considered the Sun-Mercury-satellite in the model of restricted three body problem with zero eccentricity. Here continuation method have been used to obtain the halo orbits around the Libration points L_1 and L_2 . We observe that the frequencies remain constant throughout the time interval using wavelet transform. The ridge plot at the initial guess confirms the periodicity of the halo orbits.

Keywords

Wavelet transform;Restricted three body problem; Photogravitational; Halo orbits.

AMS Subject Classification

70F15, 70F07.

[1] *Department of Mathematics, Chatra College, Chatra, Jharkhand, India.*

[2] *University Department of Mathematics, Vinoba Bhave University,Hazaribag-825301, Jharkhand, India.*

***Corresponding author**: [1] hemumishra@gmail.com; [2]jhagovi@gmail.com

Article History: Received **12** December **2019**; Accepted **24** March **2020**

Contents

1. Introduction

Mercury is the fastest and smallest planet situated in the innermost region of the Solar system. Interplanetary missions to the Mercury have become a topic of debate after Mariner 10 and MESSENGER's exploration. On 20th October 2018, Bepicolombo was launched to do the comprehensive study of Mercury. It will study the magnetic field, magnetosphere, surface and internal structure of Mercury which could reveal the origin and evolution of planets in Solar system formation. Halo orbits is a three-dimensional periodic orbit about the libration points. A. C. Clarke pointed out the importance of L_2. According to him we can relay earth based program to another side of the Moon through trans-lunar libration point L_2 [1].The idea of Clarke was overwhelming but one more question was still unanswered i.e. in which trajectory we can put our communication satellite? This question was solved in 1968 by R. Farquhar. He investigated some trajectories around L_2 and named it as halo orbits. According to his idea one can establish a continuous link from Earth to another side of Moon through establishing a communication satellite in the halo orbits around L_2. [2]. Nowadays people are interested in the halo orbits of the CR3BP (Circular Restricted Three-Body Problem), particularly halo orbits around L1 and L2. The libration point L_1, L_2 are considered as the boundary point where the gravitational force of the secondary body exist. Now a days L_1, L_2 points are observed as the most suitable points through which we can transfer interplanetary

spacecraft with minimum required energy. [3, 4]. Trajectories around L_1 in the Sun-Mars system in the restricted three-body problem with photo gravitational effect have been studied by [5]. They investigated that the radiation pressure makes longer the halo orbits also the radiation pressure push the halo orbits towards the sun when we increase its time period. [6] have also computed halo and Lissajous orbits. They investigated the Sun-Earth-satellite system with photogravitational effect of the Sun and oblateness of the Earth. They observed that radiation pressure and oblateness increases the time period around L_1 and decreases around L_2. [7] and [8] have nicely explained the geometry and motions at the collinear points of the centre manifold. [9] used Lissajous trajectories around L_1 and L_2 and evaluated the performance of a Lunar Global Positioning system. They also checked the applicability of Lunar global Communication system on both sides of the Moon. As we all know that there are various chaotic indicators or tools to investigate the nonlinear dynamical system i.e. the structure of the phase space. Time-frequency analysis based on wavelet transform is one of them, which deals the motion in the plane of time and frequency . Therefore the TFA (time frequency analysis) is a tool to detect the nature of the motion i.e. periodic or aperiodic. Here we solve a given mathematical model numerically. We are using time-frequency analysis based on the extraction of the instantaneous frequency.The extraction have been done from the phase of the continuous wavelet transform. The graph plotted using this method is known as ridge-plot. In ridge-plot, if frequency remains constant throughout a time interval, then we term that as a periodic trajectory. CWT (continuous wavelet transform) have two important base of analysis one is phase and another is amplitude.Analysis of frequency with time based on phase of CWT have been done by Vela-Arevalo and Marsden and also used by Gupta and Kumar. [10, 11] . Time-frequency analysis based on the amplitude of CWT can be seen in the work of Chandre et.al. and also used by Gupta and Kumar[11–13]. Restricted three body problem with zero eccentricity is a very good mathematical model of asymptotic analytic signal with phase variation. So for getting better insight of its motion we can apply time-frequency analysis based on phase of CWT. [12]. In this paper, our objective was to draw Halo orbits and analyze its stability through time-frequency analysis. Organization of this paper are as follows: In Section 2, we have described the configuration of the Sun-Mercury-satellite in the restricted three body problem with zero eccentricity. In perturbation theory, we need to approximate the periodic solutions uniformly which can remove secular terms. For this, we have used a continuation method for the computation of halo orbits which are described in Section 3. Analysis of frequency with time based on the phase of CWT have been explained in Section 4. In Section 5 we describe the results and discussion followed with conclusion of the paper in Section 6.

2. Configuration of Sun-Mercury-satellite model and Equations of Motion

In our mathematical model we have considered the circular restricted three body problem consisting of three bodies: The Sun, The Mercury and an infinitesimal mass (artificial satellite) with masses m_1, m_2,and m respectively. Here the artificial satellite is of negligible mass and is moving under the gravitational influence of the Sun and Mercury. Let (x',y',z') be the coordinates of the satellite in the sidereal system [14]. We have supposed that initially the line along Sun to Mercury is perpendicular on y' axis i.e the line along Sun to Mercury is perpendicular on $x'y'-$ plane.

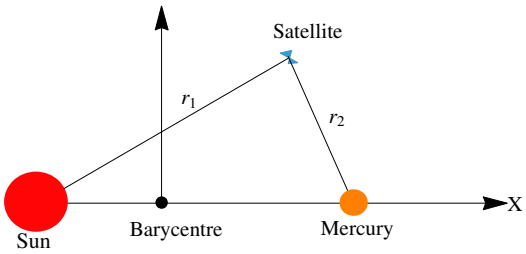

Figure 1. A Planar view of synodic coordinates (x, y, z) and sideral coordinates (x', y', z') of the satellite. The origin is located at the centre of mass of the sun and Mercury.

Let $\mu = \frac{m_2}{m_1+m_2}$ is the mass parameter and $q = 1 - \frac{F_p}{F_g}$ [15] as the mass radiation factor accounts the effect of radiation force in the system. Here the unit of length is assumed such that the constant separation of two masses is unity. The model of the problem under consideration is shown in Fig.(1). The equation of motion of for the considered model as written as [5, 16, 17]

$$\ddot{x} - 2\dot{y} = \frac{\partial U}{\partial x}, \tag{2.1}$$

$$\ddot{y} + 2\dot{x} = \frac{\partial U}{\partial y}, \tag{2.2}$$

$$\ddot{z} = \frac{\partial U}{\partial z}, \tag{2.3}$$

$$U = \frac{(x^2+y^2)}{2} + \frac{(1-\mu)q}{r_1} + \frac{\mu}{r_2}, \tag{2.4}$$

where,

$$r_1 = \sqrt{(x+\mu)^2+y^2+z^2},$$
$$r_2 = \sqrt{(x+\mu-1)^2+y^2+z^2}. \tag{2.5}$$

3. Continuation method for the halo orbits

Continuation method or Lindstedt-Poincaré method is an important technique for uniformly approximating periodic solutions which remove secular terms arising in the straightforward application of perturbation theory to weakly nonlinear problems with finite oscillatory solutions [18]. By the help of expansion theorem and the periodicity of the solution, we find convergent series approximations of periodic solutions. Here nonlinear terms alter the frequency of the linearized system [4]. [19] developed a third order periodic solution using Poincaré-Lindstedt type of successive approximations. This third order approximation provides much qualitative insight but insufficient for the serious study of proper motion near L_1 or L_2. [6] computed the halo orbit in the photogravitational Sun-earth system with oblateness using this method, extending it to fourth order by translating origin at the Lagrangian points L_1 and L_2. We have considered only the radiation effect of the Sun excluding the effect of oblateness, as it is known that in the case of the Sun-Mercury system the radiation factors is more dominant.

$$X = x+\mu \pm \gamma - 1, \quad Y = y, \quad Z = z, \tag{3.1}$$

Using the above tranlation our equations of motion 2.1-2.3 changed in the following form

$$\gamma(\ddot{X} - 2\dot{Y}) = \frac{\partial \Omega}{\partial X}, \tag{3.2}$$

$$\gamma(\ddot{Y} + 2\dot{X}) = \frac{\partial \Omega}{\partial Y}, \tag{3.3}$$

$$\gamma\ddot{Z} = \frac{\partial \Omega}{\partial Z}, \tag{3.4}$$

$$\Omega = \frac{X^2+Y^2}{2} + \frac{(1-\mu)q}{R_1} + \frac{\mu}{R_2} \tag{3.5}$$

and R_1 and R_2 changed to following form

$$R_1 = \sqrt{(X\gamma+1\mp\gamma)^2 + (Y\gamma)^2 + (Z\gamma)^2},$$
$$R_2 = \sqrt{(X\gamma\mp\gamma)^2 + (Y\gamma)^2 + (Z\gamma)^2}.$$

On expanding the non-linear terms of equation 3.5, as in [20] it reduces to

$$\begin{aligned}\Omega = {} & \gamma\frac{(X^2+Y^2)}{2} + \frac{1}{\gamma^2}\left\{\frac{(1-\mu)q\gamma}{1-\gamma} + \mu\right\} \\ & + \frac{X}{\gamma^2}\left\{-\frac{(1-\mu)q\gamma^2}{(1-\gamma)^2}\right\} \\ & + \frac{(2X^2-Y^2-Z^2)}{2\gamma^2}\left\{\frac{(1-\mu)q\gamma^3}{(1-\gamma)^3}\right\} \\ & + \frac{1}{\gamma^2}\left\{\sum_{m\geqslant 3}^{\infty} C_m\rho^m P_m\left(\frac{X}{\rho}\right)\right\}.\end{aligned} \tag{3.6}$$

So, after some algebraic manipulation, equations of motion changes in the following form

$$\ddot{X} - 2\dot{Y} - (1+2C_2)X = \frac{\partial}{\partial X}\sum_{m\geqslant 3}^{\infty} C_m\rho^m P_m\left(\frac{X}{\rho}\right), \tag{3.7}$$

$$\ddot{Y} + 2\dot{X} + (C_2-1)Y = \frac{\partial}{\partial Y}\sum_{m\geqslant 3}^{\infty} C_m\rho^m P_m\left(\frac{X}{\rho}\right), \tag{3.8}$$

$$\ddot{Z} + C_2 Z = \frac{\partial}{\partial Z}\sum_{m\geqslant 3}^{\infty} C_m\rho^m P_m\left(\frac{X}{\rho}\right). \tag{3.9}$$

where,

$$C_m = \frac{1}{\gamma^3}\left\{\frac{(-1)^m q(1-\mu)\gamma^{m+1}}{(1\mp\gamma)^{m+1}} + (\pm 1)^m(\mu)\right\}, \tag{3.10}$$

where $m = 0,1,2,3,....$ Considering only linear terms the solution of linearized equations 3.7-3.9 is

$$\begin{aligned}X(t) = {} & A_{11}e^{\alpha t} + A_{22}e^{-\alpha t} + A_{33}\cos\lambda t \\ & + A_{44}\sin\lambda t,\end{aligned} \tag{3.11}$$

$$\begin{aligned}Y(t) = {} & -\kappa_1 A_{11}e^{\alpha t} + \kappa_1 A_{22}e^{-\alpha t} \\ & - \kappa_2 A_{33}\sin\lambda t + \kappa_2 A_{44}\cos\lambda t,\end{aligned} \tag{3.12}$$

$$Z(t) = A_{55}\cos\sqrt{C_2}t + A_{66}\sin\sqrt{C_2}t, \tag{3.13}$$

where A_{11}, A_{22}, A_{33}, A_{44}, A_{55}, and A_{66} are arbitrary constants whereas

$$\alpha = \sqrt{\frac{-(2-C_2)+\sqrt{9C_2^2-8C_2}}{2}},$$

$$\lambda = \sqrt{\frac{(2-C_2)+\sqrt{9C_2^2-8C_2}}{2}},$$

$$\kappa_1 = \frac{(2C_2+1)-\alpha^2}{2\alpha},$$

$$\kappa_2 = \frac{(2C_2+1)+\lambda^2}{2\lambda}.$$

In above linearized equations, two roots are real and equal with opposite signs, which give rise to a saddle point. So we take $A_{11} = A_{22} = 0$ and

$$A_{33} = -A_X\cos\phi, A_{44} = A_X\sin\phi,$$
$$A_{55} = A_Z\sin\psi, \text{ and } A_{66} = A_Z\cos\psi,$$

to switch off the real modes for bounded solution, and the linearized equations have solutions of the form [4].

$$\begin{aligned}X(t) &= -A_X\cos(\lambda t+\phi), \\ Y(t) &= \kappa A_X\sin(\lambda t+\phi), \\ Z(t) &= A_Z\sin(\sqrt{C_2}t+\psi),\end{aligned} \tag{3.14}$$

where A_X and A_Z are the amplitudes, λ and C_2 are the frequencies, ϕ and ψ are the phases of the in plane and out of plane motions respectively. The two frequencies λ and $\sqrt{C_2}$ are responsible for the halo orbits. To obtain a halo orbits we have to equate these two frequencies by introducing a frequency correct relation $\Delta = \lambda^2 - C_2$. However, we compute the orbits upto fourth order approximation with radiation pressure. To avoid secular terms which appear as a result of the successive approximation procedure, a new independent variable τ and a frequency connection ω are introduced through, $\tau = \omega t$ and truncating the equations of motion (3.7)-(3.9) at degree 4. Then the equations are written in terms of new independent variable τ as given in [6].

$$\omega^2 X'' - 2n\omega Y' - (n^2 + 2C_2)X = \frac{3}{2}C_3(2X^2 - Y^2 - Z^2) + 2C_4(2X^2 - 3Y^2 - 3Z^2)X + \frac{5}{8}C_5\left[8X^2\{X^2 - 3(Y^2+Z^2)\} + 3(Y^2+Z^2)^2\right], \quad (3.15)$$

$$\omega^2 Y'' + 2n\omega X' + (C_2 - n^2)Y = -3C_3XY - \frac{3}{2}C_4(4X^2 - Y^2 - Z^2)Y - \frac{5}{2}C_5XY(4X^2 - 3Y^2 - 3Z^2), \quad (3.16)$$

$$\omega^2 Z'' + \lambda^2 Z = -3C_3XZ - \frac{3}{2}C_4(4X^2 - Y^2 - Z^2)Z - \frac{5}{2}C_5XZ(4X^2 - 3Y^2 - 3Z^2) + \Delta Z. \quad (3.17)$$

where, $\Delta = \lambda^2 - C_2$, which is quite small and used for the frequency correction to get the halo orbit. We need to use the perturbation technique of Lindstedt-Poincaré. Here approximate solution of the non-linear problem in a neighbourhood of the equilibrium point is to be obtained. In this technique, higher order terms of the equations of motion are considered and we produce a formal series expansion of the solution of the equations of motion which have higher accuracy and then assuming the solutions for equations (3.15), (3.16), and (3.17) in the form of perturbation,

$$X(\tau) = \varepsilon X_1(\tau) + \varepsilon^2 X_2(\tau) + \varepsilon^3 X_3(\tau) + \varepsilon^4 X_4(\tau) + \ldots \quad (3.18)$$

$$Y(\tau) = \varepsilon Y_1(\tau) + \varepsilon^2 Y_2(\tau) + \varepsilon^3 Y_3(\tau) + \varepsilon^4 Y_4(\tau) + \ldots \quad (3.19)$$

$$Z(\tau) = \varepsilon Z_1(\tau) + \varepsilon^2 Z_2(\tau) + \varepsilon^3 Z_3(\tau) + \varepsilon^4 Z_4(\tau) + \ldots \quad (3.20)$$

and

$$\omega = 1 + \varepsilon\omega_1 + \varepsilon^2\omega_2 + \varepsilon^3\omega_3 + \varepsilon^4\omega_4 + \ldots. \quad (3.21)$$

Using this substitution in equation (3.15), (3.16), and (3.17) and equating the terms of $O(\varepsilon)$, $O(\varepsilon^2)$, $O(\varepsilon^3)$, and $O(\varepsilon^4)$ to obtain the first, second, third, and fourth order equations, respectively as [6, 20] with some modifications. We solve our model considering radiation pressure only whereas [6] considered radiation pressure and oblateness both.

3.1 First order equations

Now, by introducing the frequency correction term Δ, and collecting the $O(\varepsilon^1)$ from equations (3.15-3.17), the first order equations of motions are

$$X_1'' - 2Y_1' - (1+2C_2)X_1 = 0, \quad (3.22)$$

$$Y_1'' + 2X_1' + (C_2 - 1)Y_1 = 0, \quad (3.23)$$

$$Z_1'' + \lambda^2 Z_1 = 0. \quad (3.24)$$

The periodic solutions of the above equations are:

$$X_1(\tau) = -A_X\cos(\lambda\tau + \phi), \quad (3.25)$$

$$Y_1(\tau) = \kappa A_X\sin(\lambda\tau + \phi), \quad (3.26)$$

$$Z_1(\tau) = A_Z\sin(\lambda\tau + \psi). \quad (3.27)$$

3.2 Second order equations

Similarly, collecting the $O(\varepsilon^2)$ and using the values of X_1, Y_1, and Z_1, we get

$$X_2'' - 2Y_2' - (1+2C_2)X_2 = 2\omega_1\lambda A_X(\kappa - \lambda)\cos\tau_1 + \alpha_1 + \gamma_1\cos 2\tau_1 + \gamma_2\cos 2\tau_2, \quad (3.28)$$

$$Y_2'' + 2X_2' + (C_2 - 1)Y_2 = 2\omega_1\lambda A_X(\kappa\lambda - 1)\sin\tau_1 + \beta_1\sin 2\tau_1, \quad (3.29)$$

$$Z_2'' + \lambda^2 Z_2 = 2\omega_1\lambda^2 A_Z\sin\tau_2 + \delta_1\sin(\tau_1 + \tau_2) + \delta_1\sin(\tau_2 - \tau_1), \quad (3.30)$$

where coefficients are given in Appendix I

$$\tau_1 = \lambda\tau + \phi, \qquad \tau_2 = \lambda\tau + \psi,$$

To find the bounded solution we required to eliminate the secular terms $\sin\tau_1$, $\cos\tau_1$, and $\sin\tau_2$ by setting $\omega_1 = 0$. As the bounded homogeneous solution is incorporated from first order solution of equations (3.25), (3.26), and (3.27), so we have to find only particular solution of equations (3.28), (3.29), and (3.30), which is found as

$$X_2(\tau) = \rho_{20} + \rho_{21}\cos 2\tau_1 + \rho_{22}\cos 2\tau_2, \quad (3.31)$$

$$Y_2(\tau) = \sigma_{21}\sin 2\tau_1 + \sigma_{22}\sin 2\tau_2, \quad (3.32)$$

$$Z_2(\tau) = \kappa_{21}\sin(\tau_1 + \tau_2) + \kappa_{22}\sin(\tau_2 - \tau_1), \quad (3.33)$$

where coefficients are given in the Appendix I.

3.3 Third order equations

Again, collecting the $O(\varepsilon^3)$ setting $\omega_1 = 0$, using the values of X_1, Y_1, Z_1, X_2, Y_2, and Z_2, we have

$$X_3'' - 2Y_3' - (1+2C_2)X_3 = [\nu_1 + 2\omega_2 A_X\lambda(\kappa - \lambda)]\cos\tau_1 + \gamma_3\cos\tau_1 + \gamma_4\cos(2\tau_2 + \tau_1) + \gamma_5\cos(2\tau_2 - \tau_1), \quad (3.34)$$

$$Y_3'' + 2X_3' + (C_2 - 1)Y_3 = [\nu_2 + 2\omega_2\lambda A_X(\lambda\kappa - 1)]\sin\tau_1 + \beta_3\sin 3\tau_1 + \beta_4\sin(\tau_1 + 2\tau_2) + \beta_5\sin(2\tau_2 - \tau_1), \quad (3.35)$$

$$Z_3'' + \lambda^2 Z_3 = \left[\nu_3 + A_Z\left(2\omega_2\lambda^2 + \frac{\Delta}{\varepsilon^2}\right)\right]\sin\tau_2 + \delta_3\sin 3\tau_2 + \delta_4\sin(2\tau_1+\tau_2) + \delta_5\sin(2\tau_1-\tau_2), \quad (3.36)$$

where coefficients are given in the Appendix I.

In this case we cannot remove the secular term by setting the value of ω_2, to remove the secular term from equations we adjust the phases of τ_1 and τ_2, so that $\sin(2\tau_1-\tau_2)\sim\sin\tau_2$ which is done by setting the phase relation as

$$\psi = \phi + p\frac{\pi}{2}; \qquad \text{where } p = 0,1,2,3, \quad (3.37)$$

by doing so, we can remove the secular term from (3.36) for the bounded solution if

$$\left[\nu_3 + A_Z\left(2\omega_2\lambda^2 + \frac{\Delta}{\varepsilon^2}\right) + \zeta\delta_5\right] = 0, \quad (3.38)$$

where $\zeta = (-1)^p$. Equations (3.34) and (3.35) will be also affected by the above phase condition. Then the secular terms from both equations can be removed by finding a single condition from their particular solution as

$$(\nu_1 + 2\omega_2\lambda A_X(\kappa-\lambda) + \zeta\gamma_5) - \kappa(\nu_2 + 2\omega_2\lambda A_X(\kappa\lambda-1) + \zeta\beta_5) = 0, \quad (3.39)$$

from the above relation, we get

$$\omega_2 = \frac{\nu_1 - \kappa\nu_2 + \zeta(\gamma_5 - \kappa\beta_5)}{2\lambda A_X(\lambda(\kappa^2+1) - 2\kappa)}, \quad (3.40)$$

assuming these conditions the third order equations reduces to,

$$X_3'' - 2Y_3' - (1+2C_2)X_3 = \kappa\beta_6\cos\tau_1 + (\gamma_3 + \zeta\gamma_4)\cos 3\tau_1, \quad (3.41)$$

$$Y_3'' + 2X_3' + (C_2-1)Y_3 = \beta_6\sin\tau_1 + (\beta_3 + \zeta\beta_4)\sin 3\tau_1, \quad (3.42)$$

$$Z_3'' + \lambda^2 Z_3 = (-1)^{\frac{p-1}{2}}(\delta_3 - \delta_4)\cos 3\tau_1, \quad (3.43)$$

where $\beta_6 = \nu_2 + 2\omega_2\lambda A_X(\kappa\lambda - n) + \zeta\beta_5$. The solution is given by

$$X_3(\tau) = \rho_{31}\cos 3\tau_1, \quad (3.44)$$

$$Y_3(\tau) = \sigma_{31}\sin 3\tau_1 + \sigma_{32}\sin\tau_1, \quad (3.45)$$

$$Z_3(\tau) = (-1)^{\frac{p-1}{2}}\kappa_{32}\cos 3\tau_1, \quad (3.46)$$

where coefficients are given in the Appendix I.

3.4 Fourth order equations

In order to find the fourth order approximation, we first collect the $O(\varepsilon^4)$ and incorporating all the above conditions which has been used upto third order approximations, we get

$$X_4'' - 2Y_4' - (1+2C_2)X_4 = \alpha_2 + 2A_X\lambda\omega_3(\kappa-\lambda)\cos\tau_1 + \gamma_6\cos 2\tau_1 + \gamma_7\cos 4\tau_1, \quad (3.47)$$

$$Y_4'' + 2X_4' + (C_2-1)Y_4 = 2A_X\lambda\omega_3(\kappa\lambda - 1)\sin\tau_1 + \beta_7\sin 2\tau_1 + \beta_8\sin 4\tau_1, \quad (3.48)$$

$$Z_4'' + \lambda^2 Z_4 = \alpha_3 + 2\lambda^2 A_Z\omega_3\cos\tau_1 + \delta_6\cos 2\tau_1 + \delta_7\cos 4\tau_1, \quad (3.49)$$

In the above equations the coefficients are different for different phase relation defined as $\psi = p\frac{\pi}{2} + \phi$. Here in our case we have taken $p = 1$ for simplicity. These coefficients are given in Appendix I. Here we remove the secular terms $\sin\tau_1$, and $\cos\tau_1$ by setting $\omega_3 = 0$, and assuming this we get solutions as

$$X_4(\tau) = \rho_{40} + \rho_{41}\cos 2\tau_1 + \rho_{42}\cos 4\tau_1, \quad (3.50)$$

$$Y_4(\tau) = \sigma_{41}\sin 2\tau_1 + \sigma_{42}\sin 4\tau_1, \quad (3.51)$$

$$Z_4(\tau) = \kappa_{40} + \kappa_{41}\cos 2\tau_1 + \kappa_{42}\cos 4\tau_1, \quad (3.52)$$

where coefficients are given in the Appendix I.

3.5 The final approximation

Finally, we combine all the solutions considering the mapping as $A_X \longmapsto \frac{A_X}{\varepsilon}$ and $A_Z \longmapsto \frac{A_Z}{\varepsilon}$ to remove ε from all the solutions of equations upto fourth order approximations. Combining all solutions components wise in (3.18), (3.19), and (3.20), we get

$$X(\tau) = (\rho_{20} + \rho_{31} + \rho_{40}) - A_X\cos\tau_1 + (\rho_{21} + \zeta\rho_{22} + \rho_{41})\cos 2\tau_1\cos 3\tau_1 + \rho_{42}\cos 4\tau_1, \quad (3.53)$$

$$Y(\tau) = (\kappa A_X + \sigma_{32})\sin\tau_1 + (\sigma_{21} + \sigma_{41} + \zeta\sigma_{22})\sin 2\tau_1 + \sigma_{31}\sin 3\tau_1 + \sigma_{42}\sin 4\tau_1, \quad (3.54)$$

$$Z(\tau) = (-1)^{\frac{p-1}{2}}A_Z\cos\tau_1 + (-1)^{\frac{p-1}{2}}(\kappa_{21}\cos\tau_1 + \kappa_{22} + \kappa_{32}\cos 3\tau_1) + \kappa_{40} + \kappa_{41}\cos 2\tau_1 + \kappa_{42}\cos 4\tau_1. \quad (3.55)$$

4. Time-frequency analysis based on phase of continuous wavelet transform

In this method, we extract instantaneous frequency using phase method. Details of this method can be seen in the work of [11, 21]. The wavelet transform is defined in terms of a function ψ, called the mother wavelet, in the following way

$$L_\Psi f(a,b) = \frac{1}{\sqrt{a}}\int_{-\infty}^{\infty} f(t)\bar{\Psi}\left(\frac{t-b}{a}\right)dt \quad (4.1)$$

We have chosen mother wavelet as Morlet Grossman wavelet for this computation. It can be expressed as

$$\Psi(t) = \frac{1}{\sigma\sqrt{2\Pi}}e^{i2\Pi\eta t}e^{-\frac{t^2}{2\sigma^2}} \quad (4.2)$$

The wavelet transform depends on two parameters: (a,b) where a is called the scale and is the multiple of the inverse of the frequency and b is the time parameter that slides the wavelet as a time window. The transform depends on η which is the center frequency of the wavelet:

$$\eta = \frac{1}{2\pi}\int_{-\infty}^{\infty} \omega|\hat{\psi}_{a,b}(\omega)|^2 d\omega \tag{4.3}$$

where $\psi_{a,b}(t) = b^{\frac{-1}{2}}(\psi^{\frac{(t-a)}{b}}$ and $\hat{\psi}$ denotes the Fourier transform of ψ. The time frequency representation is obtained by the relation between the scale a and the frequency $\xi = \frac{\eta}{b}$. The wavelet transform produces a common surface between a and b known as normalized Scalogram is expressed as

$$P_w f(a,\xi = \frac{\eta}{b}) = \frac{1}{b}|Wf(a,b)|^2 \tag{4.4}$$

Also we observe that $P_w f(a,-\xi) = P_w f(a,\xi)$. Thus for the computation of wavelet decomposition, we consider the positive frequency part of the time -frequency plane.
Note: The parameter η and σ can be tuned to improve the resolution. In our case $\eta = 0.8$ and $\sigma = 1$ serves the purpose. Here due to the part $(\frac{t-b}{a})$ the length of the window in wavelet transform change according to frequency. Due to this unique feature i.e. the capability of adaptation of time window according to frequency range gives better localization in frequency and time.
The wavelet transform of f provides the expansion in terms of basis function. Let Ψ_{ab} be the basis function constructed from dilations and translations of the mother wavelet Ψ:

$$\Psi_{ab} = \frac{1}{\sqrt{a}}\int_{-\infty}^{\infty} f(t)\,\Psi\left(\frac{t-b}{a}\right)dt \quad b \in \Re, a > 0.$$

$$L_\Psi f(a,b) = \langle f, \Psi_{a,b}\rangle = \frac{1}{\sqrt{a}}\int_{-\infty}^{\infty} f(t)\,\bar{\Psi}\left(\frac{t-b}{a}\right)dt.$$

Let $f(t) = A_f(t)\exp[i\Phi_\Psi(t)]$ be an analytic signal. If the wavelet Ψ is an analytic itself, then it can be expressed as

$$\Psi(t) = A_\Psi(t)\exp[i\Phi_\Psi(t)]$$

Thus

$$L_\Psi f(a,b) = \frac{1}{\sqrt{a}}\int_{-\infty}^{\infty} M_{ab}(t)\,exp[i\Phi_{ab}(t)]dt.$$

where

$$M_{ab} = A_f(t)A_\Psi\left(\frac{t-b}{a}\right)$$
$$\Phi_{ab}(t) = \Phi_f - \Phi_\Psi\left(\frac{t-b}{a}\right) \tag{4.5}$$

Let t_0 be a unique point such that $\dot{\Phi}_{ab}(t_0) = 0$ and $\ddot{\Phi}_{t_0} \neq 0$. t_0 is called stationary point. By using stationary phase approximation method, the asymptotic expression for $L_\Psi f(a,b)$ as

$$L_\Psi f(a,b) \approx \frac{1}{\sqrt{a}} f(t_0)\,\bar{\Psi}\left(\frac{t_0-b}{a}\right)\sqrt{\frac{2\Pi}{|\ddot{\Phi}_{ab}(t_0)|}}e^{i\dot{\Phi}_{ab}(t_0)\frac{\Pi}{4}} \tag{4.6}$$

Also $t_0(a,b) = b$ gives a curve in the time scale plane. Here we define the ridge of wavelet transform. The ridge of wavelet transform is the collection of points for which $t_0(a,b) = b$. From the equation $\dot{\Phi}_{ab}(t_0) = 0$, we have

$$\dot{\Phi}_{ab}(t_0) = \dot{\Phi}_f(t_0) - \frac{1}{a}\dot{\Phi}_\Psi\left(\frac{t_0-b}{a}\right) = 0$$

Then points on ridge satisfy

$$a =: a_r(b) = \frac{\dot{\Phi}_\Psi(0)}{\dot{\Phi}_f(b)}$$

Therefore instantaneous frequency $\dot{\Phi}_f(b)$ of the function f can be obtained from this equation once we have the ridge of the wavelet transform. We use the ridge extraction programs based on the phase of continuous wavelet transform given in Wavelab Package [22].
Ridge-extraction based on the phase of continuous wavelet transform can be studied in [23]. As we know, in case of Circular Restricted Three-Body Problem motion along z-axis is oscillatory, and it is totally governed by the motion along the $x-y$-axis. So, the instantaneous frequency $\omega_1(t)$ extracted from the signal made from z-coordinate and the instantaneous frequency $\omega_2(t)$ extracted from the signal made from x,y coordinates in synodic frame are exactly same.

$$Z_1(t) = X_1(t) + \imath Y_1(t) = \exp^{(-\imath t)}(x_1(t) + \imath y1(t)) \tag{4.7}$$

$$Z_2(t) = X_2(t) + \imath Y_2(t) = z_1(t) + \imath H(z_1(t)) \tag{4.8}$$

where H represents Hilbert transform of z(t) [10].

5. Results and Discussion

After making this signal we apply phase method to extract $\omega_1(t)$ from $Z_1(t)$ and $\omega_2(t)$ from $Z_2(t)$. We can decide the behaviour of signal once ridge plot is obtained. If frequency remains constant throughout the time interval then the orbit is periodic otherwise it is aperiodic.

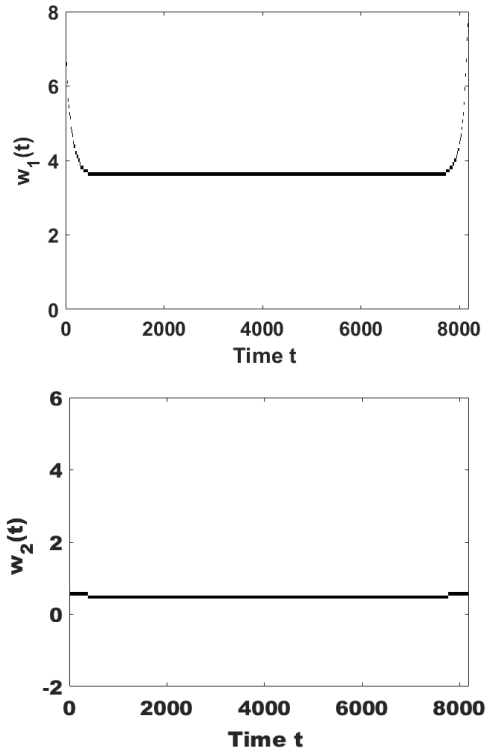

Figure 2. Ridge plot of the periodic trajectory at initial condition (0.994315, 3.82657×10^{-24}, 0.00101036, 0, 8.37179×10^{-12}, 0).

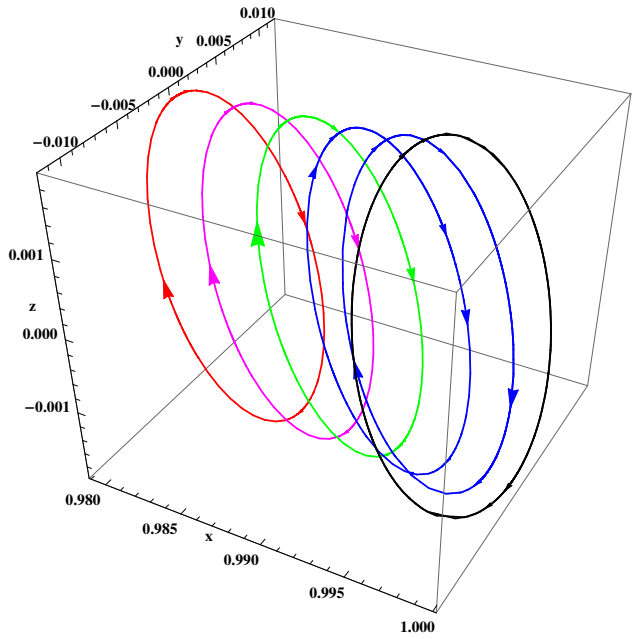

Figure 3. Halo orbit around L_1

The halo orbits for the classical case upto third order approximation in the Sun-Earth system are discussed by [20] and [4]. However, here we find the halo orbits for the classical case and considering the Sun-Mercury system with radiation pressure upto fourth order approximation using Lindstedt-Poincaré method. Using the above equations (3.53), (3.54), and (3.55) and here we take the amplitudes, $A_X = 200000$km and $A_Z = 110000$km. The 3D-halo orbits for classical case, when $q = 1$ with black color (Fig.3), time period for the motion around L_1 is 42.34days and in 5 the black color orbit around L_2 is 42.57days. The other orbits with blue to red colors shows the 3D-halo orbits, when $q = 0.99$, 0.98, 0.97, 0.96 and 0.95 respectively. The red color orbit in both the Figs.3 and 5 shows when $q = 0.95$. The variation of some parameters and time period with radiation factor q for the motion around L_1 and L_2 are given Tables 1 and 2 respectively. The time period of the halo orbits around L_1 increases whereas decreases in the case of L_2 with the increase in the radiation factor. The effect on the halo orbit due to radiation pressure of the Sun are clearly visible in Fig.3-5, that the orbits are shifting towards the Sun position. Fig.4 indicates that the eccentricity of orbit increases around L_1 with increase in radiation factor whereas in case of orbits around L_2 it decreases as shown in Fig.6.

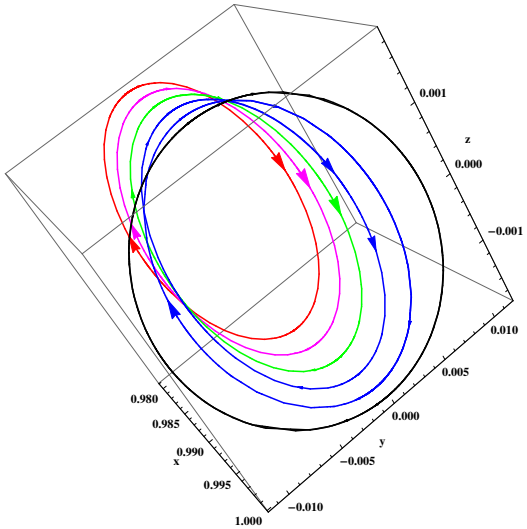

Figure 4. Halo orbit around L_1 showing the increase in eccentricity due to radiation pressure

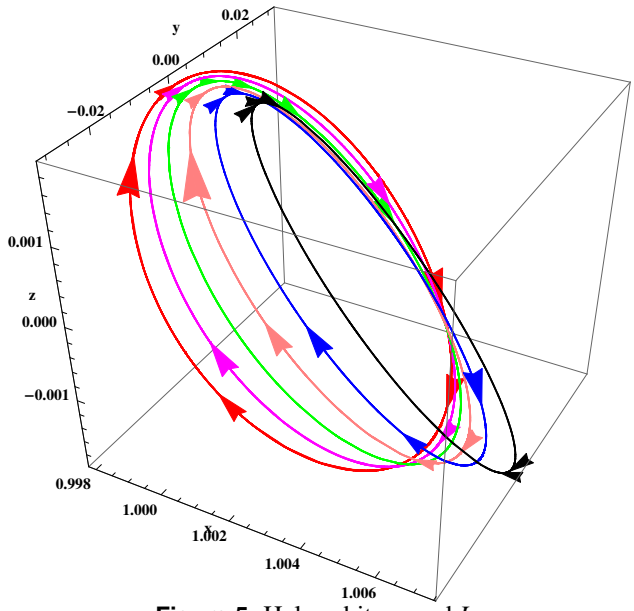

Figure 5. Halo orbit around L_2

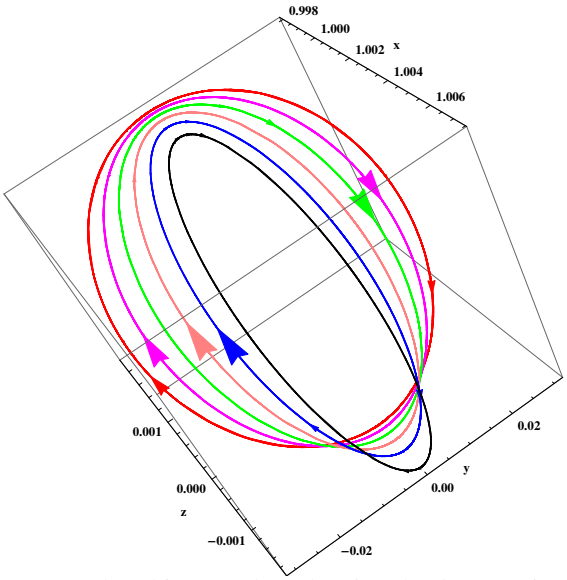

Figure 6. Halo orbit around L_2 showing the decrease in eccentricity due to radiation pressure

6. Conclusion

We have analytically computed halo orbits in Sun-Mercury-satellite system. Here we have analyzed the effect of radiation pressure on the orbits at different values on the line shown by [6].

The result shows that the radiation pressure increases the time period of the orbits around L_1 and increases the eccentricity of the orbits around L_1. With the effect of radiation pressure the halo orbits shifting towards the Sun.

Similarly, we have observed that the radiation pressure decreases the time period of the orbits around L_2 but decreases the eccentricity of the orbits. With the radiation effect, the orbits shift towards the Sun. Sometimes it preferred to have the numerical justification of the results obtained analytically. Therefore the time-frequency analysis method is implemented to confirm the results obtained. In this case, We have considered initial condition of an halo orbit obtained by the Lindstedt-Poincaré method (0.994315, 3.82657×10^{-24}, 0.00101036, 0, 8.37179×10^{-12}, 0). At this initial condition, we numerically integrate the equations of motions and finally make a signal with the help of solutions as illustrated earlier.

In Fig. 2. We have presented the ridge-plot. In ridge-plot it evident that instantaneous frequency is constant throughout the time interval considered. Thus we conclude that the orbit is periodic.

The behavior of ridge plot is in confirmation with the result obtained analytically. We have two halo orbits, but we have shown one plot to avoid redundancy.

Acknowledgments:

We are thankful to Dr.Badam singh Kusvah, Dr.Rishikesh Dutta Tiwary, Department of Applied Mathematics, IIT(ISM), Dhanbad and Dr. Vinay Kumar, Department of Mathematics, Zakir Husain College, University of Delhi, for their valuable suggestions and support in preparing this manuscript.

Table 1. The effect of radiation pressure around Lagrangian point L_1:

q	L_1	γ	C_2	C_3	C_4	C_5	λ	$\tau(dimensionless)$	$\tau(days)$
1.00	0.996194	0.00380	4.02298	3.00761	3.01149	3.01147	2.07720	3.02484	42.34
0.99	0.99469	0.00531	2.11693	1.10564	1.11104	1.11101	1.53625	4.08995	57.26
0.98	0.99234	0.00765	1.37278	0.36218	0.36998	0.36992	1.23942	5.06947	70.97
0.97	0.98940	0.10594	1.14163	0.12880	0.13964	0.13953	1.11088	5.65606	79.18
0.96	0.98619	0.13805	1.06394	0.04904	0.06325	0.06305	1.05611	5.94336	83.29
0.95	0.98285	0.17141	1.03352	0.01549	0.03325	0.03294	1.03111	6.09364	85.31

Table 2. The effect of radiation pressure around Lagrangian point L_2:

q	L_2	γ	C_2	C_3	C_4	C_5	λ	$\tau(dimensionless)$	$\tau(days)$
1.00	1.00381	0.00381	3.97726	−2.99237	2.98863	−2.98861	2.06603	3.04119	42.57
0.99	1.00296	0.00296	7.32058	−6.34225	6.33935	−6.33934	2.76267	2.27432	31.84
0.98	1.00247	0.00246	12.03570	−11.06531	11.06290	−11.06290	3.51514	1.78796	25.02
0.97	1.00214	0.00213	17.92510	−16.96340	16.96131	−16.96130	4.27212	1.47078	20.59
0.96	1.00191	0.00190	24.83041	−23.87717	23.87590	−23.87590	5.01595	1.25269	17.53
0.95	1.00174	0.00173	32.63520	−31.69180	31.69011	−31.69010	5.74142	1.09436	15.32

7. Appendix I

$$
\begin{aligned}
\alpha_1 &= \frac{3}{4}C_3[A_X^2(2-\kappa^2)-A_Z^2]\\
\gamma_1 &= \frac{3}{4}C_3A_X^2(2+\kappa^2)\\
\gamma_2 &= \frac{3}{4}C_3A_Z^2\\
\beta_1 &= \frac{3}{2}C_3\kappa A_X^2\\
\delta_1 &= \frac{3}{2}C_3A_XA_Z\\
\rho_{20} &= -\frac{\alpha_1}{(1+2C_2)},\\
\rho_{21} &= \frac{4\lambda\beta_1-\gamma_1(4\lambda^2+1-C_2)}{(1-4\lambda^2)^2+(1+4\lambda^2-2C_2)C_2},\\
\rho_{22} &= -\frac{\gamma_2(1+4\lambda^2-C_2)}{(1-4\lambda^2)^2+(1+4\lambda^2-2C_2)C_2},\\
\sigma_{21} &= \frac{4\lambda\gamma_1-\beta_1(1+4\lambda^2+2C_2)}{(1-4\lambda^2)^2+(1+4\lambda^2-2C_2)C_2},\\
\sigma_{22} &= \frac{4\lambda\gamma_2}{(1-4\lambda^2)^2+(1+4\lambda^2-2C_2)C_2},\\
\kappa_{21} &= -\frac{\delta_1}{3\lambda^2}, \qquad \kappa_{22}=\frac{\delta_1}{\lambda^2}.\\
\nu_1 &= -\frac{3}{2}C_3[A_X(4\rho_{20}+2\rho_{21}+\kappa\sigma_{21})+A_Z(\kappa_{21}\\
&\quad +\kappa_{22})]+\frac{3}{2}C_4A_X[A_X^2(\kappa^2-2)+2A_Z^2],\\
\nu_2 &= -\frac{3}{2}C_3A_X[2\kappa\rho_{20}-\kappa\rho_{21}-\sigma_{21}]+\frac{3}{2}C_4A_X\kappa\\
&\quad [A_X^2\left(\frac{3}{4}\kappa^2-1\right)+\frac{A_Z^2}{2}],\\
\nu_3 &= \frac{3}{2}C_3[A_X(\kappa_{21}+\kappa_{22})+A_Z(\rho_{22}-2\rho_{20})]\\
&\quad +\frac{3}{4}C_4A_Z[A_X^2\left(\frac{\kappa^2}{2}-2\right)+\frac{3}{4}A_Z^2],\\
\gamma_3 &= -\frac{3}{2}C_3A_X(2\rho_{21}-\kappa\sigma_{21})-\frac{1}{2}C_4A_X^3(2+3\kappa^2),\\
\gamma_4 &= \frac{3}{2}C_3(\kappa A_X\sigma_{22}+A_Z\kappa_{21}-2A_X\rho_{22})-\frac{3}{2}C_4A_XA_Z^2,\\
\gamma_5 &= -\frac{3}{2}C_3(2A_X\rho_{22}+\kappa A_X\sigma_{22}-A_Z\kappa_{22})-\frac{3}{2}C_4A_XA_Z^2,\\
\beta_3 &= \frac{3}{2}C_3A_X(\sigma_{21}-\kappa\rho_{21})-\frac{3}{8}C_4\kappa A_X^3(\kappa^2+4),\\
\beta_4 &= \frac{3}{2}C_3A_X(\sigma_{22}-\kappa\rho_{22})-\frac{3}{8}C_4\kappa A_XA_Z^2,\\
\beta_5 &= \frac{3}{2}C_3A_X(\sigma_{22}+\kappa\rho_{22})+\frac{3}{8}C_4\kappa A_XA_Z^2,\\
\delta_3 &= -\frac{3}{8}(A_Z^3C_4+4A_ZC_3\rho_{22}),\\
\delta_4 &= -\frac{3}{2}C_3(A_Z\rho_{21}-A_X\kappa_{21})-\frac{3}{8}C_4A_X^2A_Z(\kappa^2+4),\\
\delta_5 &= \frac{3}{2}C_3(A_Z\rho_{21}-A_X\kappa_{22})+\frac{3}{8}C_4A_ZA_X^2(\kappa^2+4).\\
\rho_{31} &= \frac{6\lambda(\beta_3+\zeta\beta_4)-(1+9\lambda^2-C_2)(\gamma_3+\zeta\gamma_4)}{(1-9\lambda^2)^2+(1+9\lambda^2-2C_2)C_2},\\
\sigma_{31} &= \frac{6\lambda(\gamma_3+\zeta\gamma_4)-(1+9\lambda^2+2C_2)(\beta_3+\zeta\beta_4)}{(1-9\lambda^2)^2+(1+9\lambda^2-2C_2)C_2},\\
\sigma_{32} &= -\frac{\kappa\beta_6}{2\lambda},\\
\kappa_{31} &= -\frac{(\delta_3+\delta_4)}{8\lambda^2},\\
\kappa_{32} &= \frac{\delta_3-\delta_4}{8\lambda^2}.\\
\rho_{40} &= -\frac{\alpha_2}{1+2C_2},\\
\rho_{41} &= \frac{4\beta_7+(-1-4\lambda^2+C_2)\gamma_6}{(1-4\lambda^2)^2+(1+4\lambda^2-2C_2)C_2},\\
\rho_{42} &= \frac{8\beta_8+(-1-16\lambda^2+C_2)\gamma_7}{(1-16\lambda^2)^2+(1+16\lambda^2-2C_2)C_2},\\
\sigma_{41} &= -\left(\frac{\beta_7+4\lambda\rho_{41}}{1+4\lambda^2-C_2}\right),\\
\sigma_{42} &= -\left(\frac{\beta_8+8\lambda\rho_{42}}{1+16\lambda^2-C_2}\right),\\
\kappa_{40} &= \frac{\alpha_3}{\lambda^2},\\
\kappa_{41} &= \frac{-\delta_6}{3\lambda^2},\\
\kappa_{42} &= \frac{-\delta_7}{15\lambda^2}.\\
\alpha_2 &= \frac{3}{64}(5C_5((3\kappa^4-8\kappa^2+8)A_X^4+2(\kappa^2-12)A_X^2A_Z^2\\
&\quad +3A_Z^4)-32C_4(-2A_XA_Z(\kappa_{21}+2\kappa_{22})+A_Z^2(2\rho_{20}\\
&\quad +\rho_{21}-\rho_{22})+A_X^2(2(\kappa^2-2)\rho_{20}-(\kappa^2+2)\rho_{21}\\
&\quad +2\rho_{22}+\kappa^2\rho_{22}-2\kappa(\sigma_{21}-\sigma_{22})))-16C_3(\kappa_{21}^2\\
&\quad +2\kappa_{22}^2-4\rho_{20}^2-2(\rho_{21}-\rho_{22})^2\\
&\quad +(\sigma_{21}-\sigma_{22})^2+2\kappa A_X\sigma_{32}))\\
\gamma_6 &= -\frac{5}{16}C_5((3\kappa^4-8)A_X^4+24A_X^2A_X^2-3A_Z^4)+3C_4\\
&\quad (A_X^2((\kappa^2+2)\rho_{20}-(\kappa^2-2)(\rho_{21}-\rho_{22}))+2(\kappa_{21}\\
&\quad +\kappa_{22})A_XA_Z-(\rho_{20}+\rho_{21}-\rho_{22})A_Z^2)-\frac{3}{2}C_3(\kappa\sigma_{31}A_X\\
&\quad -\kappa\sigma_{32}A_X+2\rho_{31}A_X+\kappa_{32}A_Z+2\kappa_{21}\kappa_{22}-4\rho_{20}\rho_{21}\\
&\quad +4\rho_{20}\rho_{22})+8\lambda^2\omega_2(\rho_{21}-\rho_{22})+4\lambda\omega_2(\sigma_{21}-\sigma_{22})\\
\alpha_3 &= \frac{1}{16\varepsilon^2}(15C_5(\kappa^2-4)\varepsilon^2A_X^3A_Z+3\varepsilon^2A_XA_Z(15C_5A_Z^2\\
&\quad -4C_4(\kappa\sigma_{21}-\kappa\sigma_{22}+8\rho_{20}+4\rho_{21}-4\rho_{22}))\\
&\quad +6C_4((\kappa^2+4)\kappa_{21}-2(\kappa^2-4)\kappa_{22})\varepsilon^2A_X^2\\
&\quad -2(9C_4(\kappa_{21}+2\kappa_{22})\varepsilon^2A_Z^2+4(2\kappa_{22}(\Delta-3C_3\rho_{20}\varepsilon^2)\\
&\quad +3C_3\kappa_{21}(\rho_{22}-\rho_{21})\varepsilon^2)))
\end{aligned}
$$

$$\begin{aligned}\gamma_7 &= \frac{5}{64}C_5((3\kappa^4+24\kappa^2+8)A_X^4\\ &-6(\kappa^2+4)A_X^2A_Z^2+3A_Z^4)\\ &+\frac{3}{2}C_4(A_X^2((\kappa^2+2)\rho_{21}-(\kappa^2+2)\rho_{22}\\ &+2\kappa(\sigma_{22}-\sigma_{21}))\\ &+2\kappa_{21}A_XA_Z+(\rho_{22}-\rho_{21})A_Z^2)-\frac{3}{4}C_3(-2\kappa\sigma_{31}A_X\\ &+4\rho_{31}A_X+2\kappa_{32}A_Z+\kappa_{21}^2-2\rho_{21}^2-2\rho_{22}^2+4\rho_{21}\rho_{22}\\ &-\sigma_{21}^2-\sigma_{22}^2+2\sigma_{21}\sigma_{22})\end{aligned}$$

$$\begin{aligned}\beta_7 &= \frac{3}{2}C_3(A_X(\kappa\rho_{31}+\sigma_{31}+\sigma_{32})+2\rho_{20}(\sigma_{22}-\sigma_{21}))\\ &+\frac{3}{4}C_4(A_X^2((3\kappa^2-4)(\sigma_{21}-\sigma_{22})+8\kappa\rho_{20})\\ &+2\kappa\kappa_{22}A_XA_Z+(\sigma_{21}-\sigma_{22})A_Z^2)-\frac{5}{8}C_5\kappa A_X^2\\ &((3\kappa^2-4)A_X^2+3A_Z^2)+8\lambda^2\omega_2(\sigma_{21}-\sigma_{22})\\ &+4\lambda\omega_2(\rho_{21}-\rho_{22})\end{aligned}$$

$$\begin{aligned}\delta_6 &= \frac{1}{4\varepsilon^2}(-3\varepsilon^2A_X(-8C_4(\rho_{20}+\rho_{21}-\rho_{22})A_Z\\ &+5C_5A_Z^3-2C_3\kappa_{32})+20C_5\varepsilon^2A_X^3A_Z\\ &+3C_4((\kappa^2-4)\kappa_{21}-(\kappa^2+4)\kappa_{22})\varepsilon^2A_X^2\\ &+\kappa_{21}(9C_4\varepsilon^2A_Z^2+4(-3C_3\rho_{20}\varepsilon^2+\Delta\\ &+8\lambda^2\omega_2\varepsilon^2))+3\varepsilon^2(3C_4\kappa_{22}A_Z^2-2C_3\rho_{31}A_Z\\ &+4C_3\kappa_{22}(\rho_{22}-\rho_{21})))\end{aligned}$$

$$\begin{aligned}\delta_7 &= \frac{1}{16}(-6C_4((\kappa^2+4)\kappa_{21}A_X^2+2A_XA_Z(\kappa\sigma_{21}\\ &-\kappa\sigma_{22}-4\rho_{21}+4\rho_{22})-3\kappa_{21}A_Z^2)+5C_5A_XA_Z\\ &((3\kappa^2+4)A_X^2-3A_Z^2)+24C_3(\kappa_{32}A_X-\rho_{31}A_Z\\ &+\kappa_{21}(\rho_{22}-\rho_{21})))\end{aligned}$$

$$\begin{aligned}\beta_8 &= \frac{1}{16}(5C_5\kappa(3\kappa^2+4)A_X^4-3A_X^2(5C_5\kappa A_Z^2+2C_4\\ &((3\kappa^2+4)(\sigma_{21}-\sigma_{22})-8\kappa\rho_{21}+8\kappa\rho_{22}))\\ &+12A_X(C_4\kappa\kappa_{21}A_Z+2C_3(\sigma_{31}-\kappa\rho_{31}))+6(\sigma_{21}\\ &-\sigma_{22})(C_4A_Z^2+4C_3(\rho_{22}-\rho_{21})))\end{aligned}$$

References

[1] ARTHUR C Clarke. i—the dynamics of space flight. *The Journal of Navigation*, 3(4):357–364, 1950.

[2] R.W. Farquhar. *The Control and Use of Libration-point Satellites*. Department of Aeronautics and Astronautics, Stanford University, 1968.

[3] W. S. Koon, M. W. Lo, J. E. Marsden, and S. D. Ross. Low Energy Transfer to the Moon. *Celestial Mechanics and Dynamical Astronomy*, 81:63–73, 2001.

[4] W.S. Koon, M.W. Lo, and J.E. Marsden. *Dynamical Systems: The Three-body Problem and Space Mission Design*. Interdisciplinary Applied Mathematics. Springer-Verlag New York Incorporated, 2011.

[5] R. T. Eapen and R. K. Sharma. Mars interplanetary trajectory design via Lagrangian points. *Astrophysics and Space Science*, 353:65–71, September 2014.

[6] R. D. Tiwary and B. S. Kushvah. Computation of halo orbits in the photogravitational Sun-Earth system with oblateness. *Astrophysics and Space Science*, 357:73, May 2015.

[7] G. Gomez, A. Jorba, J. Masdemont, and C. Simo. Study of the transfer from the Earth to a halo orbit around the equilibrium point L1. *Celestial Mechanics and Dynamical Astronomy*, 56:541–562, August 1993.

[8] À. Jorba and J. Masdemont. Dynamics in the center manifold of the collinear points of the restricted three body problem. *Physica D Nonlinear Phenomena*, 132:189–213, July 1999.

[9] D. Romagnoli and C. Circi. Lissajous trajectories for lunar global positioning and communication systems. *Celestial Mechanics and Dynamical Astronomy*, 107:409–425, August 2010.

[10] Luz V Vela-Arevalo and Jerrold E Marsden. Time–frequency analysis of the restricted three-body problem: transport and resonance transitions. *Classical and Quantum Gravity*, 21(3):S351, 2004.

[11] Beena R Gupta and Vinay Kumar. Characterization of the phase space structure of circular restricted three-body problem: An alternative approach. *International Journal of Bifurcation and Chaos*, 26(02):1650029, 2016.

[12] C. Chandre, S. Wiggins, and T. Uzer. Time–frequency analysis of chaotic systems. *Physica D: Nonlinear Phenomena*, 181(3):171 – 196, 2003.

[13] Beena R Gupta and Vinay Kumar. Time-frequency analysis of asymmetric triaxial galaxy model including effect of spherical dark halo component. *International Journal of Astronomy and Astrophysics*, 5(02):106, 2015.

[14] C. D. Murray and S. F. Dermott. *Solar System Dynamics*. UK: Cambridge University Press, 2000, February 2000.

[15] J. A. Burns, P. L. Lamy, and S. Soter. Radiation forces on small particles in the solar system. *Icarus*, 40:1–48, October 1979.

[16] S. W. McCuskey. *Introduction to celestial mechanics*. Addison-Wesley Pub. Co., 1963.

[17] R. K. Sharma. The linear stability of libration points of the photogravitational restricted three-body problem when the smaller primary is an oblate spheroid. *Astrophysics and Space Science*, 135:271–281, July 1987.

[18] Ferdinand Verhulst. *Nonlinear differential equations and dynamical systems*. Springer Science & Business Media, 2006.

[19] D. L. Richardson. Analytic construction of periodic orbits about the collinear points. *Celestial Mechanics*, 22:241–253, October 1980.

[20] Robert Thurman and Patrick A. Worfolk. The geometry of halo orbits in the circular restricted three-body problem. Technical report, University of Minnesota: Geometry Center Research Report GCG95, 1996.

[21] Luz V Vela-Arevalo and Jerrold E Marsden. Time–frequency analysis of the restricted three-body problem: transport and resonance transitions. *Classical and Quantum Gravity*, 21(3):S351–S375, jan 2004.

[22] *WAVELAB 850*.

[23] Stéphane Mallat. *A wavelet tour of signal processing*. Elsevier, 1999.

★★★★★★★★★
ISSN(P):2319 – 3786
Malaya Journal of Matematik
ISSN(O):2321 – 5666
★★★★★★★★★